NACA

RESEARCH MEMORANDUM

AERODYNAMIC CHARACTERISTICS OF A CRUCIFORM-WING MISSILE

WITH CANARD CONTROL SURFACES AND OF SOME VERY SMALL

SPAN WING-BODY MISSILES AT A MACH NUMBER OF 1.41

By M. Leroy Spearman and Ross B. Robinson

Langley Aeronautical Laboratory
Langley Field, Va.

NATIONAL ADVISORY COMMITTEE
FOR AERONAUTICS
WASHINGTON
April 12, 1954

NACA RM L54B11 ~~CONFIDENTIAL~~

NATIONAL ADVISORY COMMITTEE FOR AERONAUTICS

RESEARCH MEMORANDUM

AERODYNAMIC CHARACTERISTICS OF A CRUCIFORM-WING MISSILE

WITH CANARD CONTROL SURFACES AND OF SOME VERY SMALL

SPAN WING-BODY MISSILES AT A MACH NUMBER OF 1.41

By M. Leroy Spearman and Ross B. Robinson

SUMMARY

An investigation has been made to determine the aerodynamic characteristics of a cruciform 70° delta-wing missile configuration with 70° delta canard control surfaces at $M = 1.41$ in the Langley 4- by 4-foot supersonic pressure tunnel. The complete model, various combinations of component parts, and modifications to the basic configuration were tested through an angle-of-attack range of 0° to about 28° at a sideslip angle of 0° and through an angle-of-sideslip range of 0° to about 20° at an angle of attack of 0°. Modifications to the configuration included variation of the body length and canard area and the substitution of a series of very small span wings for the cruciform delta wings and canard controls.

The cruciform, canard-type missile with optimum center-of-gravity location had a maximum trim angle of attack of about 16° with a horizontal-canard deflection of 12°. The short body (fineness ratio of 15.7) with the very small span wing indicated the possibility of obtaining low static margin and high maneuverability for the optimum center-of-gravity location.

INTRODUCTION

In connection with the development of missile configurations with canard control surfaces, an investigation has been conducted in the Langley 4- by 4-foot supersonic pressure tunnel to determine the longitudinal and lateral aerodynamic characteristics of a series of such configurations. The models had cruciform wings and canard controls of delta plan form with 70° swept leading edges and were equipped with all-movable canard surfaces for both pitch and yaw control and movable wing-tip ailerons for roll control.

~~CONFIDENTIAL~~

The results of an investigation of the effects of body length (fineness ratios of 14.8, 15.7, 16.7, 17.7, and 19.1) on the longitudinal stability and control characteristics of these missiles at a Mach number of 2.01 are presented in reference 1. The aerodynamic characteristics of the canard surfaces in the presence of the fineness ratio 19.1 body at a Mach number of 1.61 are presented in reference 2. The results of an investigation made at a Mach number of 2.01 to determine the effects of large deflections of the canard control and deflections of the wing-tip controls on the aerodynamic characteristics of the fineness ratio 15.7 configuration are presented in reference 3.

Some of these configurations were selected for further tests at a Mach number of 1.41 and the results are presented herein. The basic configuration was a canard-type cruciform wing arrangement with a body fineness ratio of 15.7. Various component parts, including the body alone, the body-wing combination, and the body-canard combination, were investigated. In addition, the effect of varying the canard size was investigated on the body alone and on the complete model.

Further modifications included the addition of narrow full-length longitudinal strips, simulating very small span wings, along the center line of the body-alone configuration for both the fineness ratio 15.7 body and a fineness ratio 19.1 body. These strips were added in an effort to improve the linearity of the normal-force and pitching-moment coefficients at higher angles of attack by altering the body crossflow characteristics. In addition, this small-span type of lifting surface is of current interest as a means of alleviating the problem of missile stowage in military aircraft.

SYMBOLS

The results of the tests are presented as standard NACA coefficients of forces and moments referred to the body axis system (fig. 1) with the moment reference point for all configurations located 6.25 body diameters forward of the base of the body (-19.5 percent of the wing mean aerodynamic chord). All coefficients, including those for the configurations with the small span wing, are based on the total area of the cruciform delta wing resulting from extending the wing leading and trailing edges to the body center line.

C_N — normal-force coefficient (N/qS)

C_c — chord-force coefficient (C/qS)

C_m — pitching-moment coefficient $(M'/qS\bar{c})$

C_Y lateral-force coefficient, Y/qS

C_l rolling-moment coefficient, $L/qS\bar{c}$

C_n yawing-moment coefficient, $N'/qS\bar{c}$

L/D lift-drag ratio

N normal force

C chord force

M' pitching moment

Y lateral force

L' rolling moment

M Mach number

N' yawing moment

p_0 stagnation pressure

q free-stream dynamic pressure

S total wing area resulting from extending wing leading edge
          and trailing edge to body center line

$\bar{c}$ wing mean aerodynamic chord

d diameter of body

b span of wing

l length of body

x distance from nose along body center line

Δx longitudinal shift in moment reference point, positive rearward

α angle of attack, deg

β angle of sideslip, deg

ϕ angle of roll, deg

δ_H horizontal-canard deflection angle

$S_{c_{exp}}/S_{w_{exp}}$ ratio of exposed area of canard surface to exposed wing area

MODELS AND APPARATUS

Sketches of the models are shown in figure 2. The geometric characteristics of the models are presented in table I.

The body of the model was composed of a parabolic nose followed by the frustum of a cone which was faired into a cylinder. The body length was varied through the use of different lengths of the cylindrical portion. Resulting body fineness ratios were 15.7 and 19.1. Coordinates of the body are given in table II. The canard surfaces and the wing had delta plan forms with 70° swept leading edges and hexagonal sections. The ratio of exposed canard area to exposed wing area for the basic configuration was 0.10. The horizontal canard was motor driven and deflections could be set by remote control; the vertical-canard deflections were set manually. A series of thin longitudinal strips simulating very small span wings (b/d ratios of 1.19, and 1.38) were tested on the fineness ratio 15.7 body. The small-span wings having b/d ratios of 1.19, 1.38, and 2.05 were tested on the fineness ratio 19.1 body. Details of these configurations are shown in figure 2. The small span wings were attached in the horizontal plane only.

Force measurements were made through the use of a 6-component internal strain-gage balance. The model was mounted in the tunnel on a remotely controllable rotary-type sting. The angle-of-attack range was from 0° to about 28° at roll angles of 0° and 90°. The angle-of-sideslip range was from 0° to about 20°.

TESTS, CORRECTIONS, AND ACCURACY

The conditions for the tests were:

Mach number 1.41
Stagnation temperature, $^{\circ}F$ 100
Stagnation pressures, lb/sq in. abs . . . . 4.0 and 10.7
Reynolds numbers, based on $\bar{c}$ . . . . 1.17 $\times$ 10^6 and 3.13 $\times$ 10^6

The stagnation dewpoint was maintained sufficiently low (-25°F or less) so that no condensation effects were encountered in the test section.

The angle of attack and angle of sideslip were corrected for the deflection of the balance and sting under load. The Mach number variation in the test section was approximately ±0.01 and the flow-angle variation in the vertical and horizontal planes did not exceed about ±0.1°. No corrections were applied to the data to account for these flow variations. The base pressure was measured and the chord force was adjusted to a base pressure equal to the free-stream static pressure.

The estimated errors (including calibration errors, zero shift, instrument error, and repeatability) in the individual measured quantities are as follows:

Stagnation pressure, p_o, lb/sq in. abs	Error in -					
	C_N	C_c	C_m	C_Y	C_l	C_n
10.7	±0.006	±0.003	±0.0006	±0.0015	±0.0006	±0.0007
4.0	±.015	±.007	±.0015	±.004	±.0015	±.0018

Both the angle of attack and angle of sideslip are estimated to be correct within ±0.1°.

RESULTS AND DISCUSSION

Aerodynamic Characteristics of Cruciform Model and Component Parts

The aerodynamic characteristics in pitch ($\phi = 0°$) of the complete cruciform-wing model ($l/d = 15.7$) and combinations of its components are presented in the following order: body alone and body plus canards in figure 3, body plus wings in figure 4, and complete model with several values of horizontal-canard deflections in figure 5. For the moment-center location of the present tests, a maximum trim angle of attack of about 3.5° was obtained for a 12° control deflection. Deflection of the horizontal canard resulted in no apparent change in the slope of the pitching-moment curve, indicating negligible effects of the canard flow field on the wings. For the same configuration at $M = 2.01$ (ref. 1), the stability was slightly decreased and the maximum trim angle of attack was about 4°. The aerodynamic characteristics in sideslip ($\phi = 90°$) of the complete model ($l/d = 15.7$) are presented in figure 6 for the various values of δ_H. The slightly different values of forces and moments obtained for $\phi = 0°$ and $\phi = 90°$ probably result from the different longitudinal positions of the horizontal and vertical canards. Deflection of the horizontal canard at an angle of sideslip resulted in some

induced rolling moment but had no apparent effect on C_Y and C_n. The induced rolling moments are somewhat larger than those shown and discussed in reference 3 for the same configuration at $M = 2.01$.

Effects of Canard Size

The effects of varying the area of the canards on the aerodynamic characteristics of the body-plus-canards and the complete-model configurations ($l/d = 15.7$) are shown in figures 7 and 8, respectively. These results were obtained at $\phi = 90^\circ$ (corresponding to the sideslip plane) with the vertical canard deflected as the control surface. The pitching-moment and normal-force coefficients shown were obtained from the yawing-moment and side-force measurements. The reduction in stability resulting from increasing the canard area is only slightly greater for the complete-model than for the body-canard configuration which is an indication of only a small increase in the interference effects of the canard on the wing.

Effects of Small Span Wings

The effects on the aerodynamic characteristics in pitch of adding the small span wings to the bodies are presented in figure 9. The results for the $l/d = 19.1$ body at C_N values above about 0.3 were obtained at a reduced tunnel stagnation pressure (4.0 lb/sq in. abs) because of pitching-moment limitations of the internal balance. These results are shown as dashed lines with flagged symbols in figure 9(b).

Addition of the small span wings increases the chord-force coefficient, as would be expected. No base pressure measurements were made for the $l/d = 19.1$ body alone, but it is estimated that the values of C_C for this body should be approximately the same as those shown for the $l/d = 15.7$ body alone.

Addition of the small span wings produced large increases in C_N and C_m throughout the angle-of-attack range.

Comparison of Small-Span-Wing and

Cruciform-Wing Configurations

Comparison of the values of L/D for the various small-span-wing configurations (fig. 10) indicates the expected increasing values of L/D as b/d becomes larger. Since the small-span-wing models had only two

panels, the values of L/D for these configurations are slightly opti-
mistic in comparison with the cruciform models. The L/D values for a
four-panel configuration would be only slightly lower because of the
small C_C increment due to the small span wings. For angles of attack
up to 12°, the cruciform-wing configuration maintains the higher L/D,
but above 12° there is little difference in the values of L/D for all
configurations. For small span wings with a ratio of b/d of 1.19, the
longer-body ($l/d = 19.1$) model had only slightly higher L/D than the
shorter body.

The effect on C_m of varying the center-of-gravity location for the
bodies with the small span wings is shown in figure 11. The results for
the $l/d = 15.7$ model (fig. 11(a)) indicate a more linear variation
of C_m with α than do those for the $l/d = 19.1$ model (fig. 11(b)).
For a center-of-gravity location of $x/l = 0.44$, the shorter model exhibits
a linear pitching-moment variation permitting the use of a low static
margin and it is conceivable that a small, rearward control surface might
produce high trim angles of attack and a high degree of manueverability.
Center-of-gravity locations as far forward as $x/l = 0.44$ may, however,
be difficult to achieve in actual practice.

The effect of varying the center-of-gravity location of the cruciform-
wing model (fig. 12) indicates that for $\delta_H = 12°$ the trim angle of attack
might be increased from 3.5° at $x/l = 0.60$ to 16° at $x/l = 0.68$. Such
an optimum center-of-gravity location for the cruciform-wing configuration
is, perhaps, more realistic than that required for the very small span
wing-body arrangement.

<div align="center">CONCLUSIONS</div>

An investigation has been made to determine the aerodynamic char-
acteristics at M = 1.41 of a cruciform 70° delta-wing missile configu-
ration with 70° delta canard control surfaces. Modifications to the
configuration included the substitution of a series of very small span
wings for the cruciform delta wings and canard controls. Analysis of
the results of this investigation has indicated the following conclusions:

1. For the same center-of-gravity location the cruciform-wing missile
had greater longitudinal stability and greater induced rolling moments
than was obtained at M = 2.01.

2. For the optimum center-of-gravity location, a maximum trim angle
of attack of about 16° was obtained with a control deflection of 12° for
the cruciform-wing missile.

3. The short body missile with a small span wing (ratio of span to body diameter of 1.38) with the center of gravity at 44 percent of the body length aft of the nose exhibited a nearly linear pitching-moment variation with angle of attack and indicated the possibility of obtaining a very low static margin and high maneuverability.

Langley Aeronautical Laboratory,
    National Advisory Committee for Aeronautics,
        Langley Field, Va., January 28, 1954.

REFERENCES

1. Spearman, M. Leroy: Aerodynamic Characteristics in Pitch of a Series of Cruciform-Wing Missiles With Canard Controls at a Mach Number of 2.01. NACA RM L53I14, 1953.

2. Spearman, M. Leroy: Component Tests To Determine the Aerodynamic Characteristics of an All-Movable 70° Delta Canard-Type Control in the Presence of a Body at a Mach Number of 1.61. NACA RM L53I03, 1953.

3. Spearman, M. Leroy: Effect of Large Deflections of a Canard Control and Deflections of a Wing-Tip Control on the Static-Stability and Induced-Roll Characteristics of a Cruciform Canard Missile at a Mach Number of 2.01. NACA RM L53K03, 1953.

TABLE I

GEOMETRIC CHARACTERISTICS OF MODELS

Cruciform wings:
Span, in. 11.85
Chord at body center line, in. 17.07
Chord at body intersection, in. 13.41
Area (leading and trailing edges extended to body
    body center line), sq in. 104.8
Area (exposed), sq in. 64.2
Aspect ratio 1.40
Sweep angle of leading edge, deg 70
Thickness ratio at body center line 0.0147
Leading-edge section angle normal to leading edge, deg 15.6
Trailing-edge section angle normal to trailing edge, deg . . . 7.4
Mean aerodynamic chord, in. 11.48

Canard surfaces:
Aspect ratio 1.73
Sweep angle of leading edge, deg 70
Ratio of canard exposed area to wing exposed area . . 0.05, 0.10, 0.20
Area (exposed), sq in. 3.22, 6.42, 12.84

Bodies:
Maximum diameter, in. 2.67
Base area, sq in. 5.58
Length, in. 42.00, 50.83
Fineness ratio 15.7, 19.1

Low span wings:
Thickness, in. 0.13
Width, in. 0.25, 0.50, 1.36
Ratio of span to body diameter 1.19, 1.38, 2.05
Exposed area (on short body), sq in. 20.75, 41.25
Exposed area (on long body), sq in. 25.17, 50.09, 115.02

TABLE II

BODY COORDINATES IN INCHES

Body station		Radius	
0	(Nose)	0	
.297		.076	
.627		.156	
.956		.233	
1.285		.307	
1.615		.378	
1.945		.445	
2.275		.509	
2.605		.573	
2.936		.627	
3.267		.682	
3.598		.732	
3.929		.780	
4.260		.824	
4.592		.865	
4.923		.903	
5.255		.940	
5.587		.968	
5.920		.996	
6.252		1.020	
6.583		1.042	} Conical section
11.542		1.333	
50.833		1.333	Cylindrical section
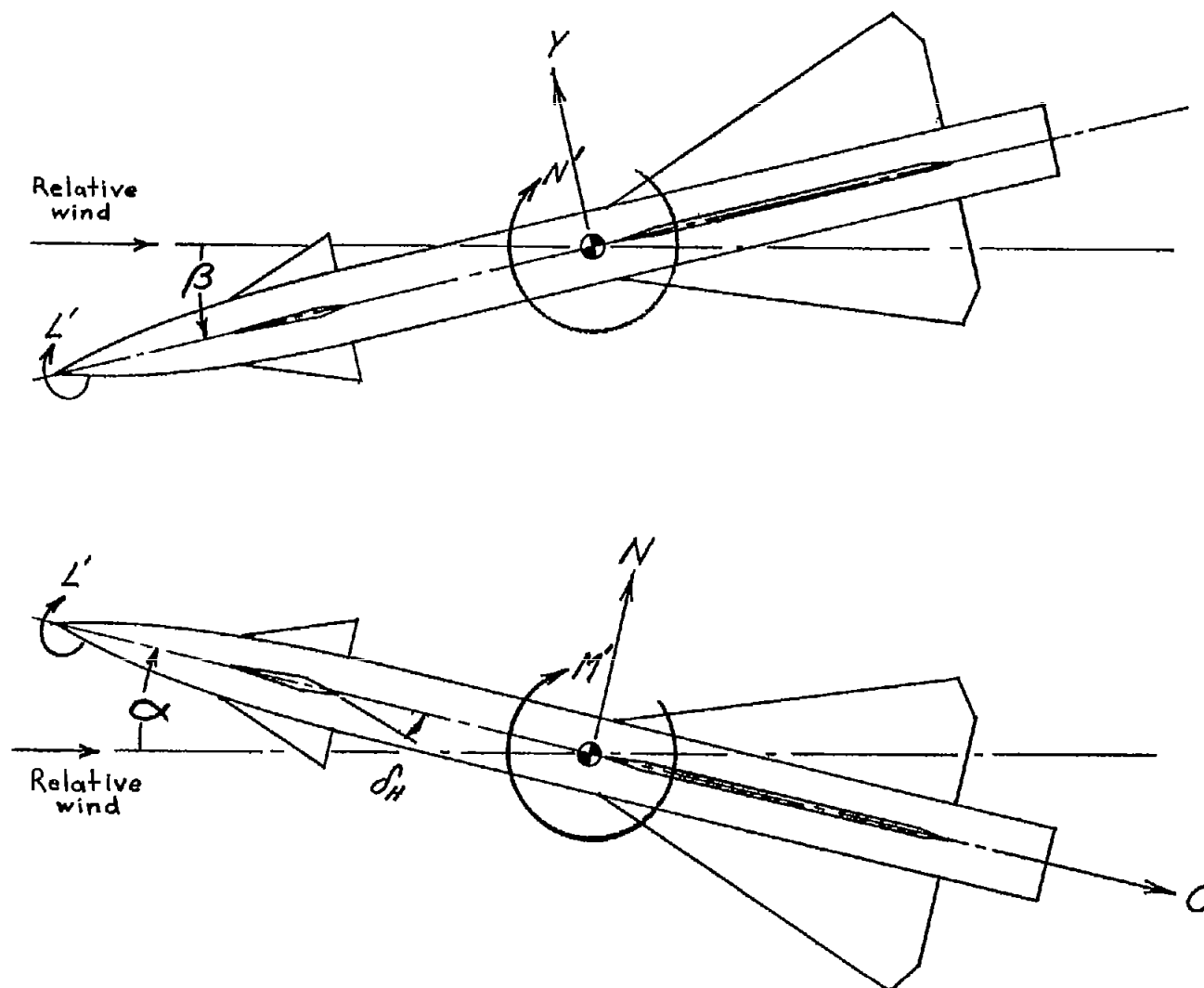
Figure 1.- System of body axes. Arrows indicate positive values.

42.00

25.33 — Moment center

2.67

Body alone

9.13 — Horizontal canard hinge line

31.11

9.46 — Vertical canard hinge line

Body + canards

2.93

11.85
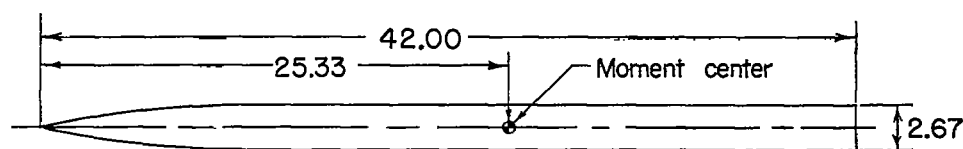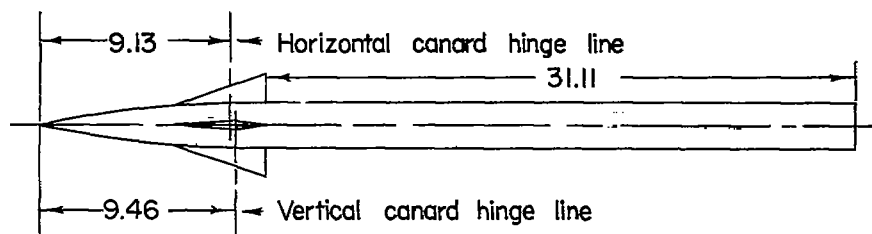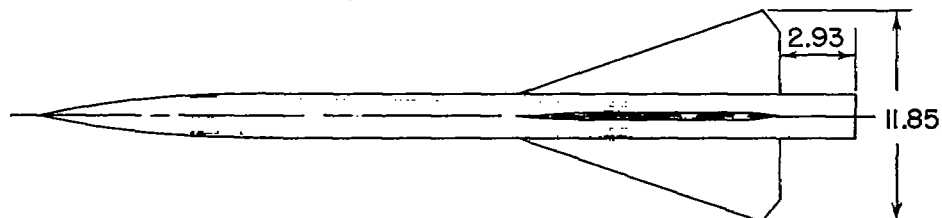
Body + wings
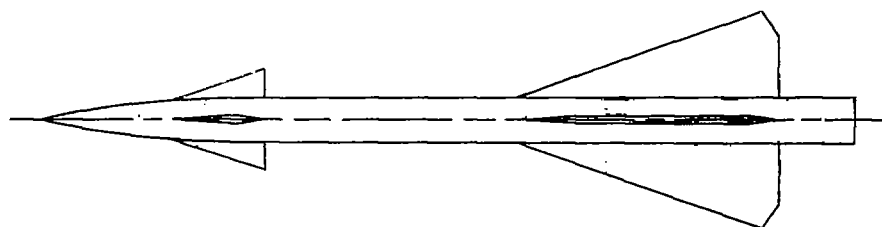
Complete model
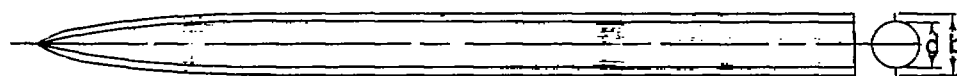
Canard span
(tip to tip)

Body + small span wings; b/d = 1.19 and 1.38

Horizontal	5.40
Vertical	4.45

(a) Short body; model 1; fineness ratio = 15.7.

Figure 2.- Plan forms of model configurations. All dimensions are in inches.

50.83

34.17

Moment center

2.67

Body alone

Body + small span wings; b/d = 1.19 and 1.38

39.95

d b

d b

Body + canard + small span wings; b/d = 2.05
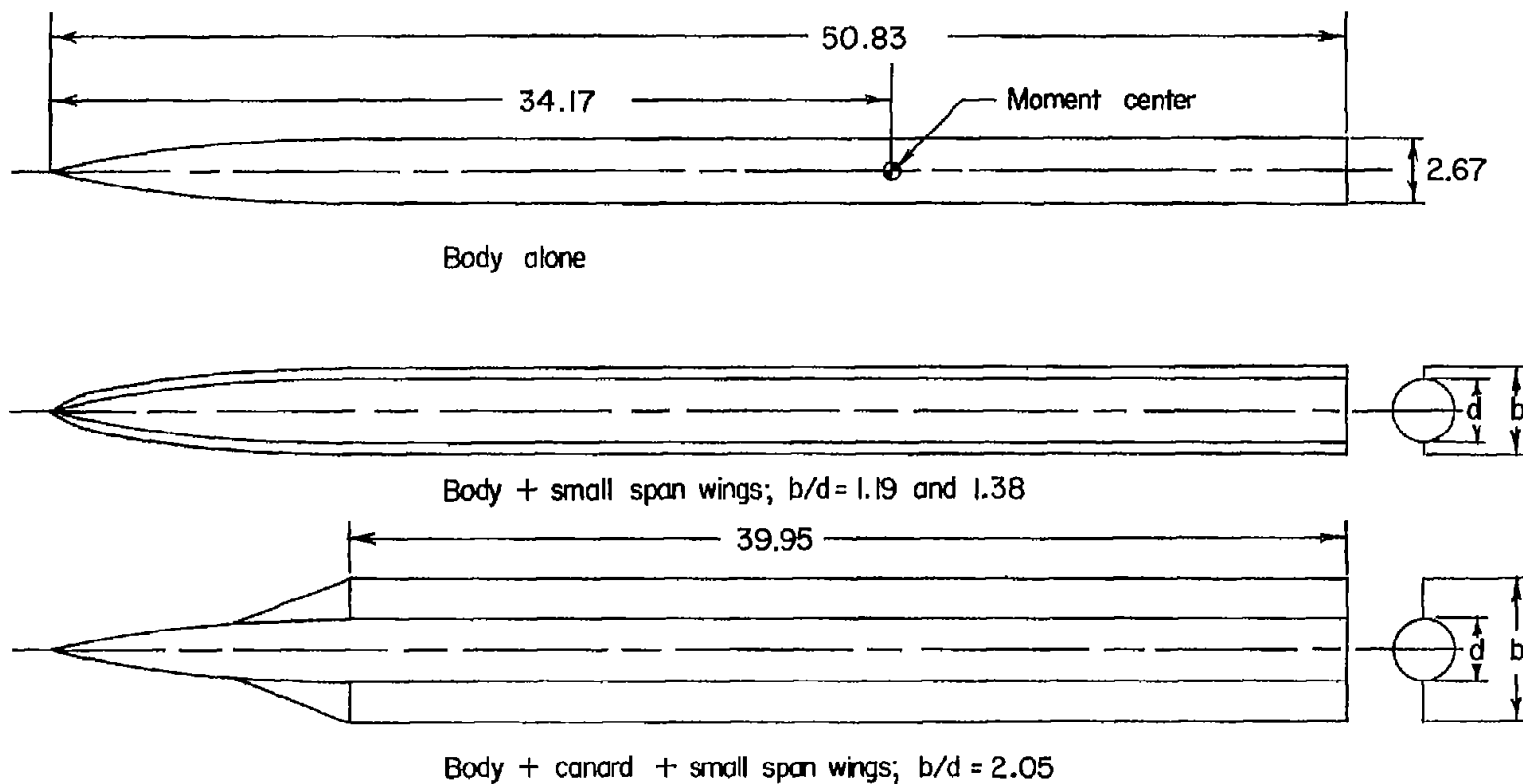
Note: Canard same size and location as horizontal canard in Figure 2a.

(b) Long body; model 2; fineness ratio = 19.1.

Figure 2.- Continued.
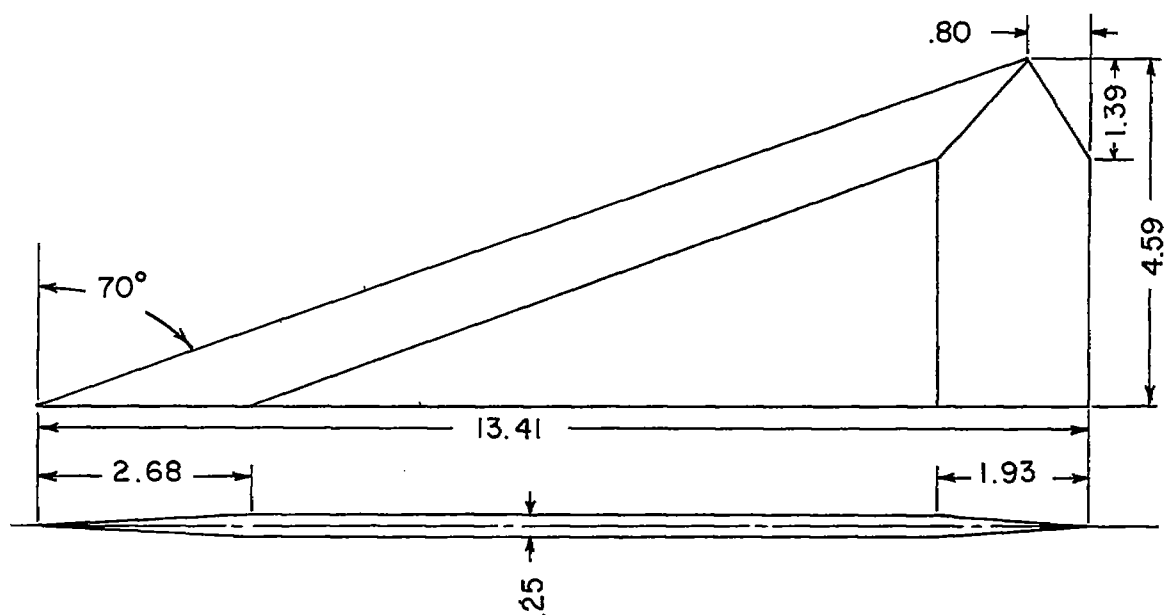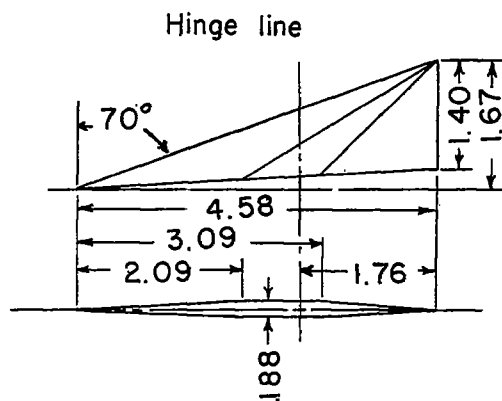
(c) Details of wing and control panels.

Figure 2.- Continued.

Hinge line

2.36

1.98

2.49

.19

1.35

4.86

6.48

Large 70° delta canard, $\dfrac{S_c}{S_w} = 0.20$

.16

1.18

1.25

.73

2.99

3.24

Small 70° delta canard, $\dfrac{S_c}{S_w} = 0.05$
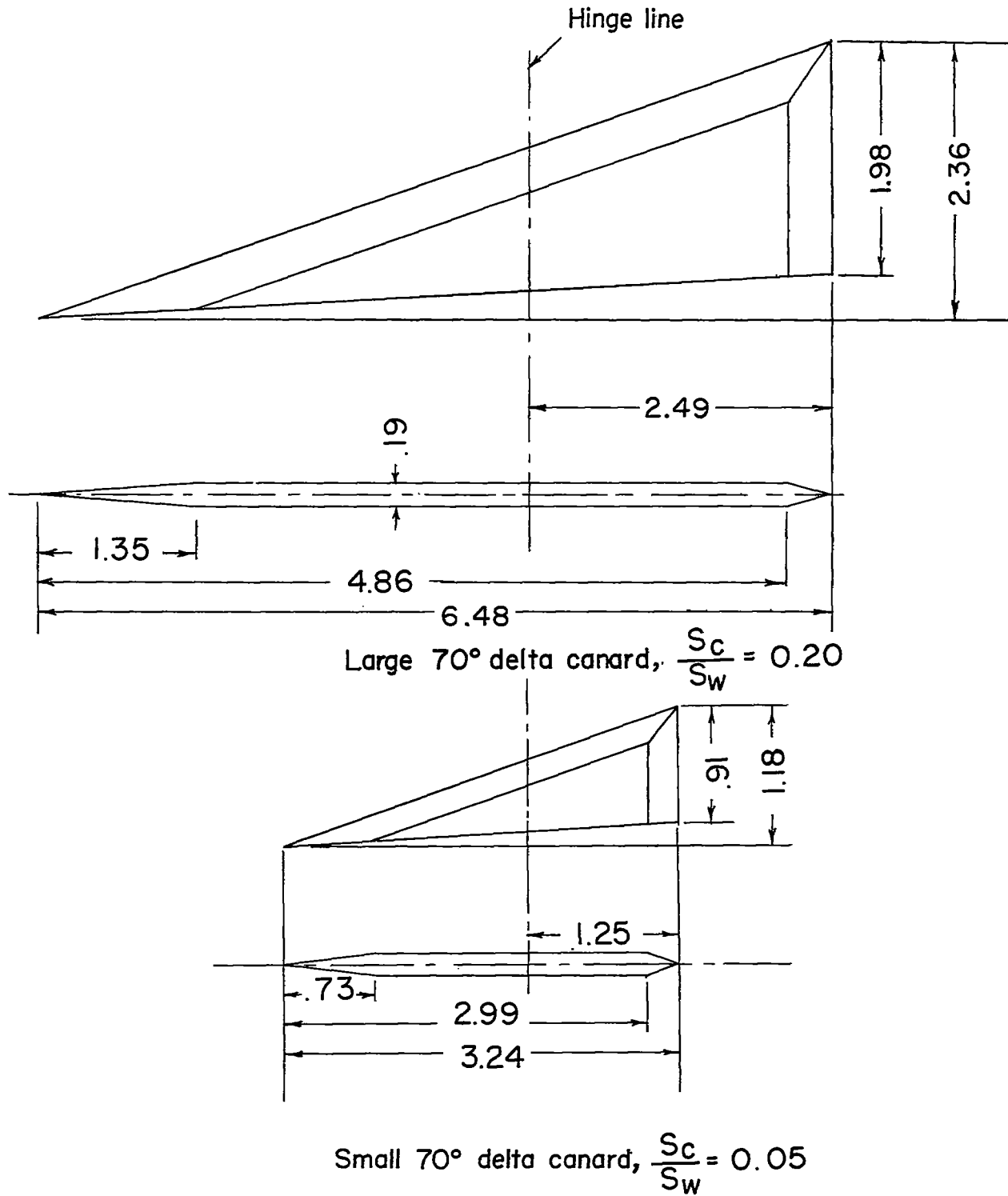
(c) Concluded.

Figure 2.- Concluded.
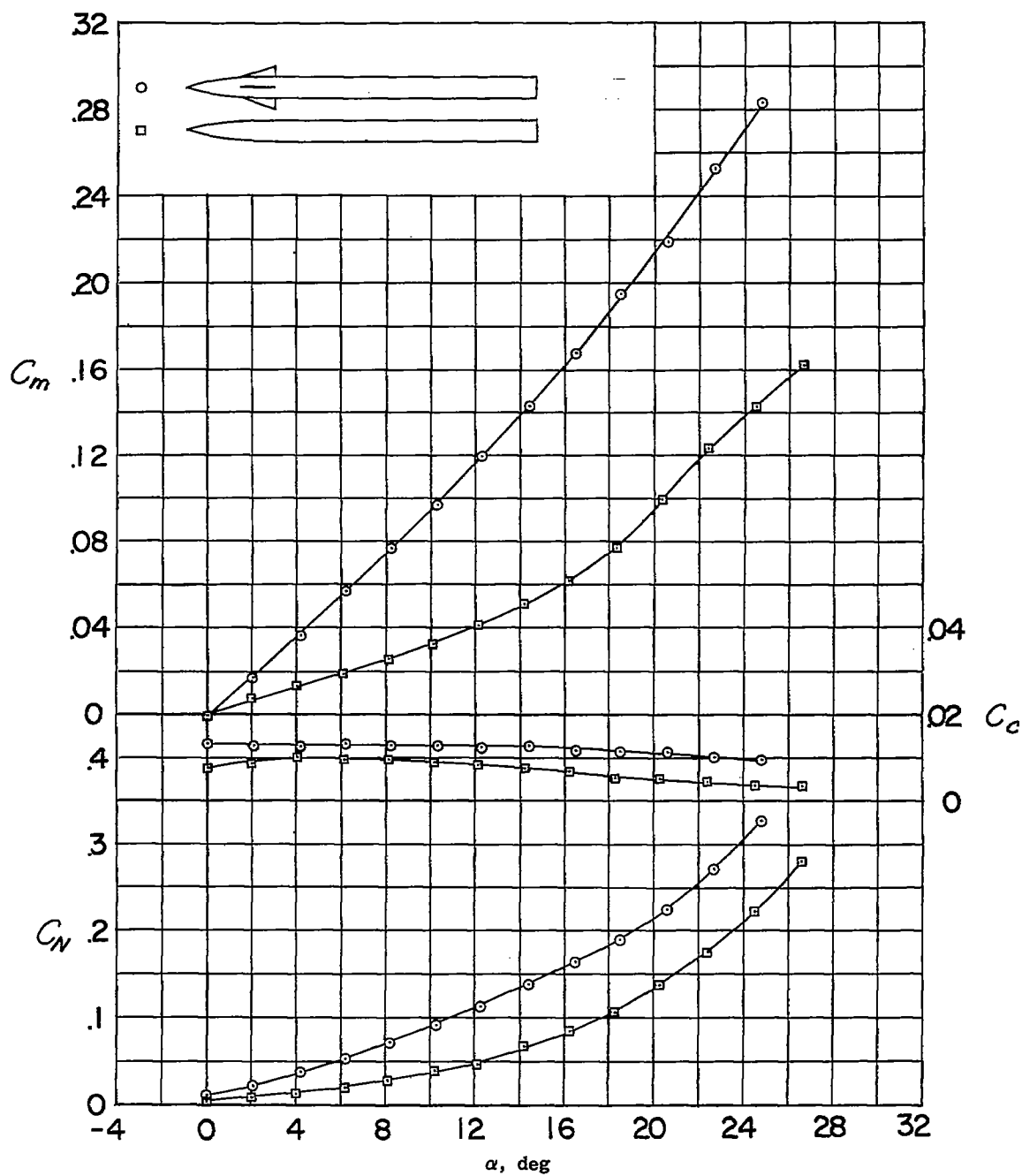
Figure 3.- Aerodynamic characteristics in pitch of the body and body plus canards. l/d = 15.7; ϕ = 0°; β = 0°; δ_H = 0°; c.g. at x/l = 0.60.

NACA RM L54B11   ~~CONFIDENTIAL~~
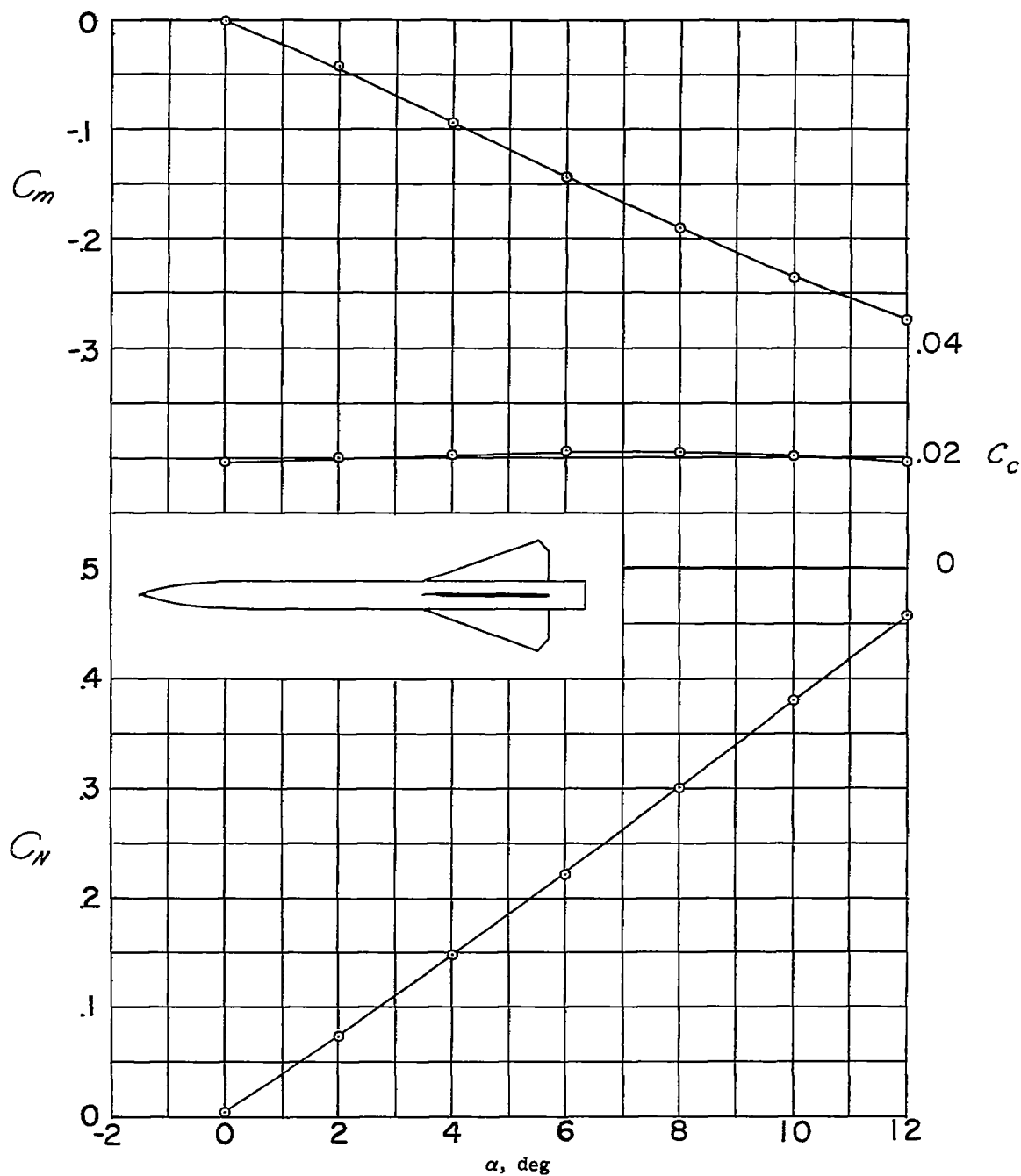
Figure 4.- Aerodynamic characteristics in pitch of the body plus wings. $l/d = 15.7$; $\phi = 0°$; $\beta = 0°$; c.g. at $x/l = 0.60$.

CONFIDENTIAL
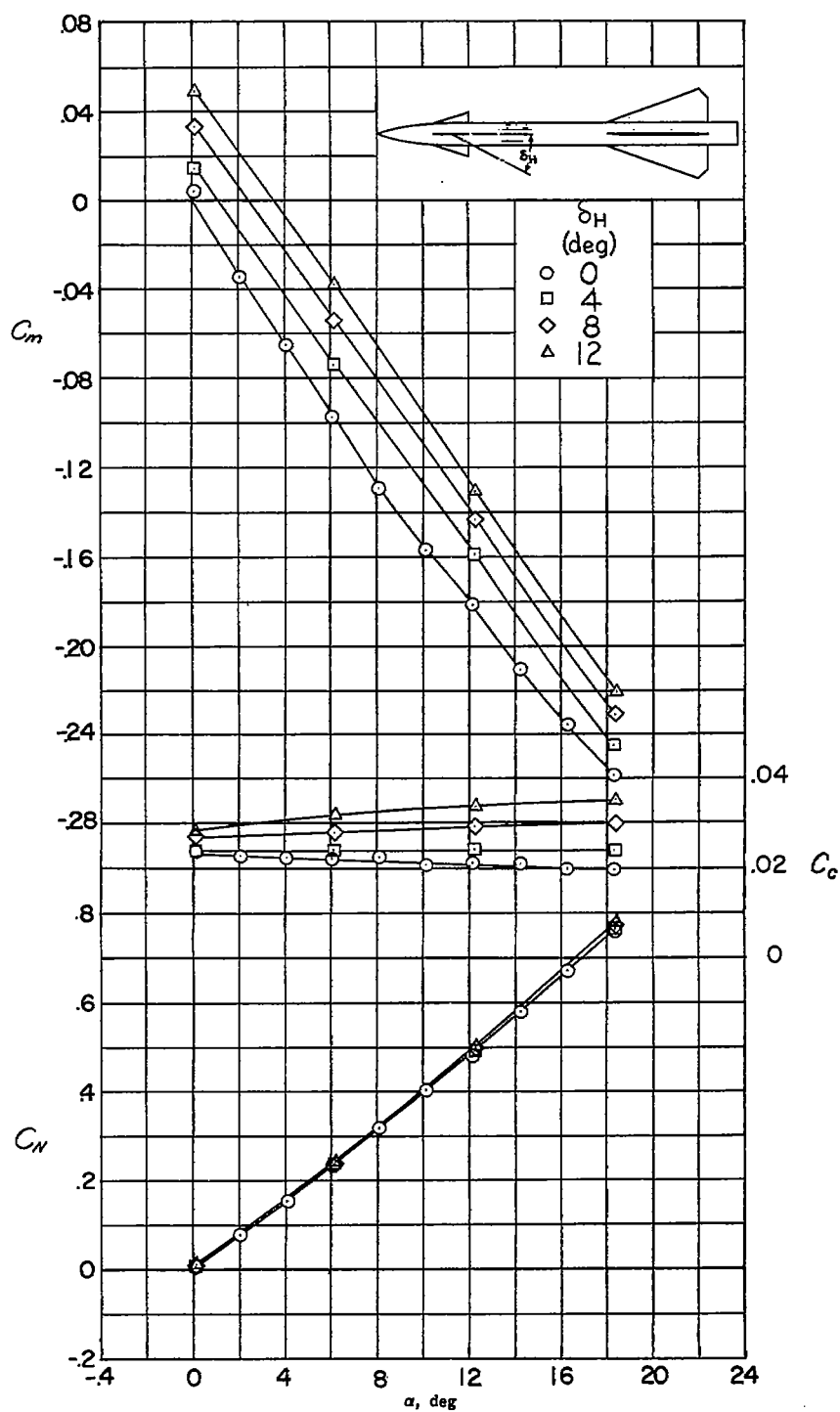
Figure 5.- Aerodynamic characteristics in pitch of the complete configuration with various deflections of horizontal canard. $l/d = 15.7$; $\phi = 0°$; $\beta = 0°$; c.g. at $x/l = 0.60$.
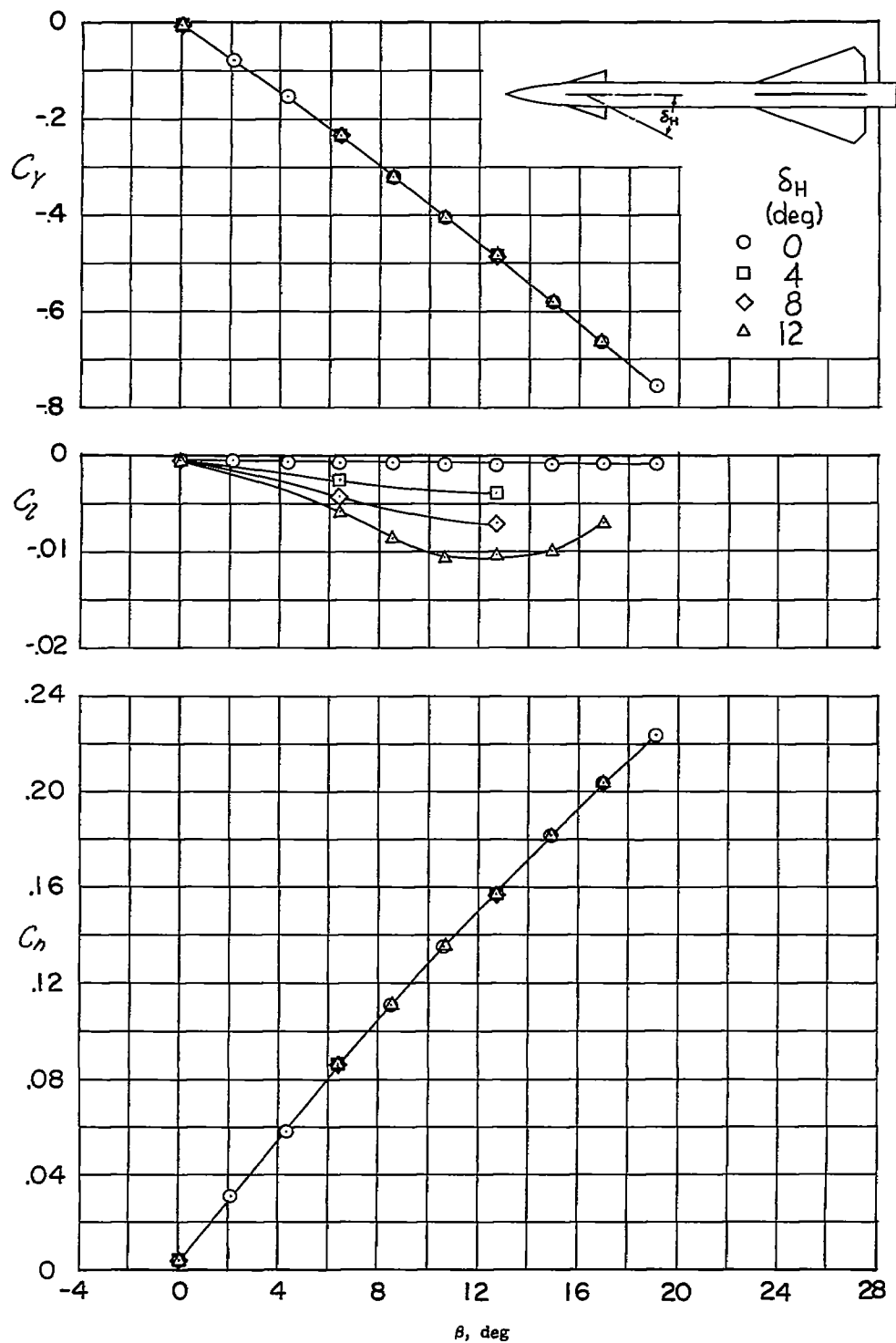
Figure 6.- Effect of horizontal-canard deflection on the lateral charac-
teristics of the complete model. $l/d = 15.7$; $\phi = 90°$; $\alpha = 0°$; c.g. at
$x/l = 0.60$.
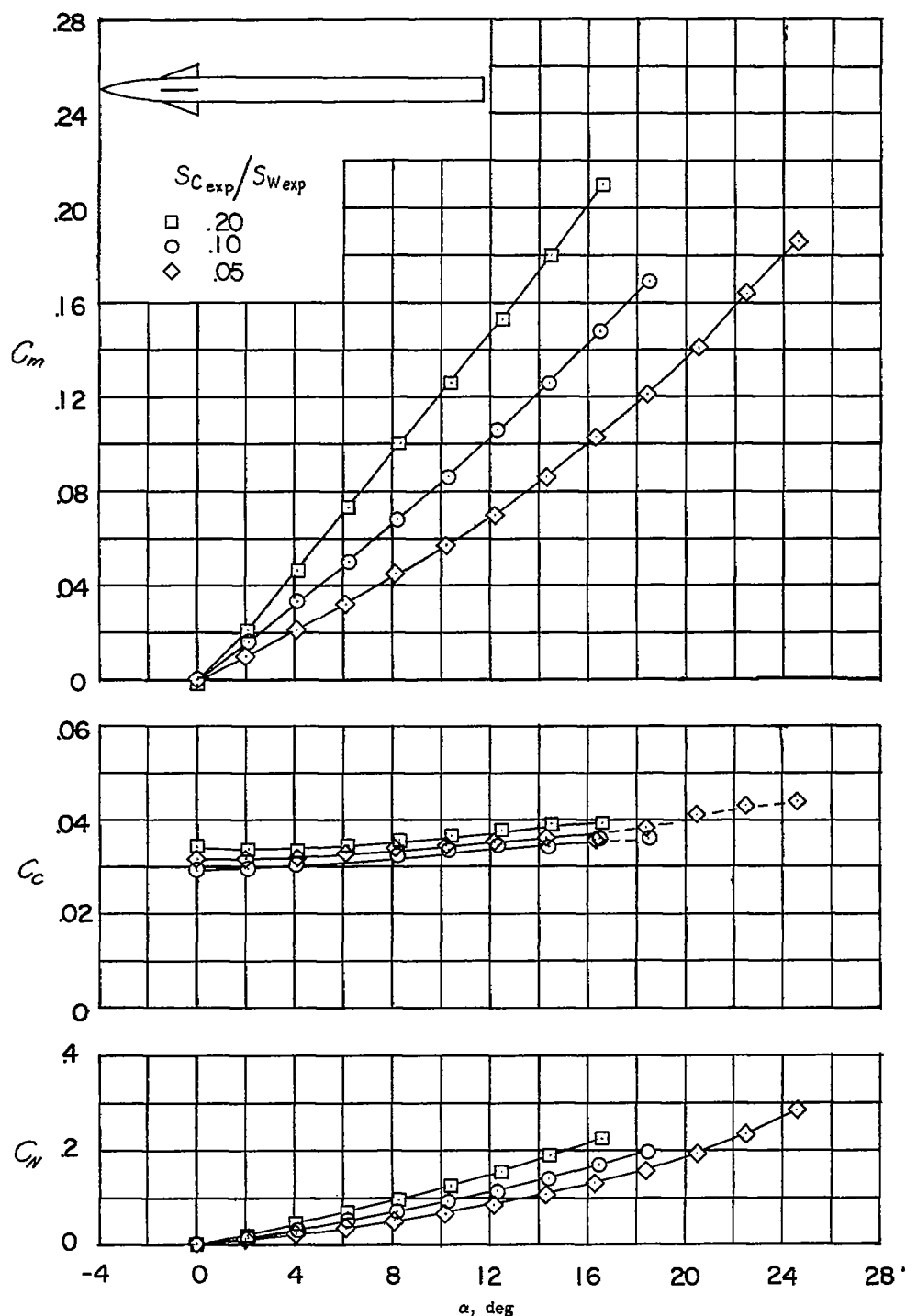
Figure 7.- Effect of canard size on aerodynamic characteristics in pitch of body-plus-canards configuration. $l/d = 15.7$; $\phi = 90°$; $\alpha = 0°$; $\delta_H = 0°$; c.g. at $x/l = 0.60$.
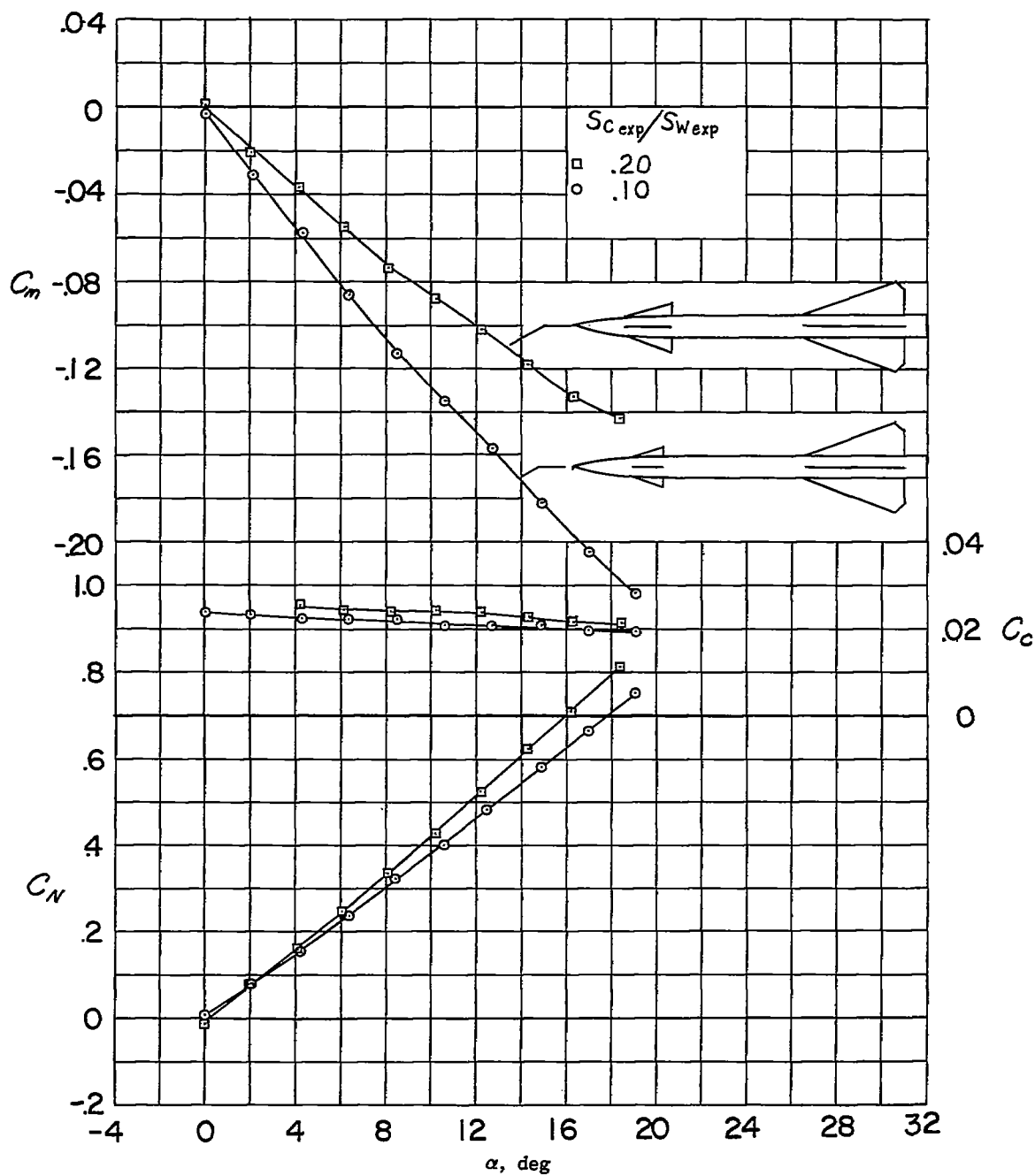
Figure 8.- Effect of canard size on aerodynamic characteristics in pitch of complete model. $l/d = 15.7$; $\phi = 90°$; $\delta_H = 0°$; c.g. at $x/l = 0.60$.
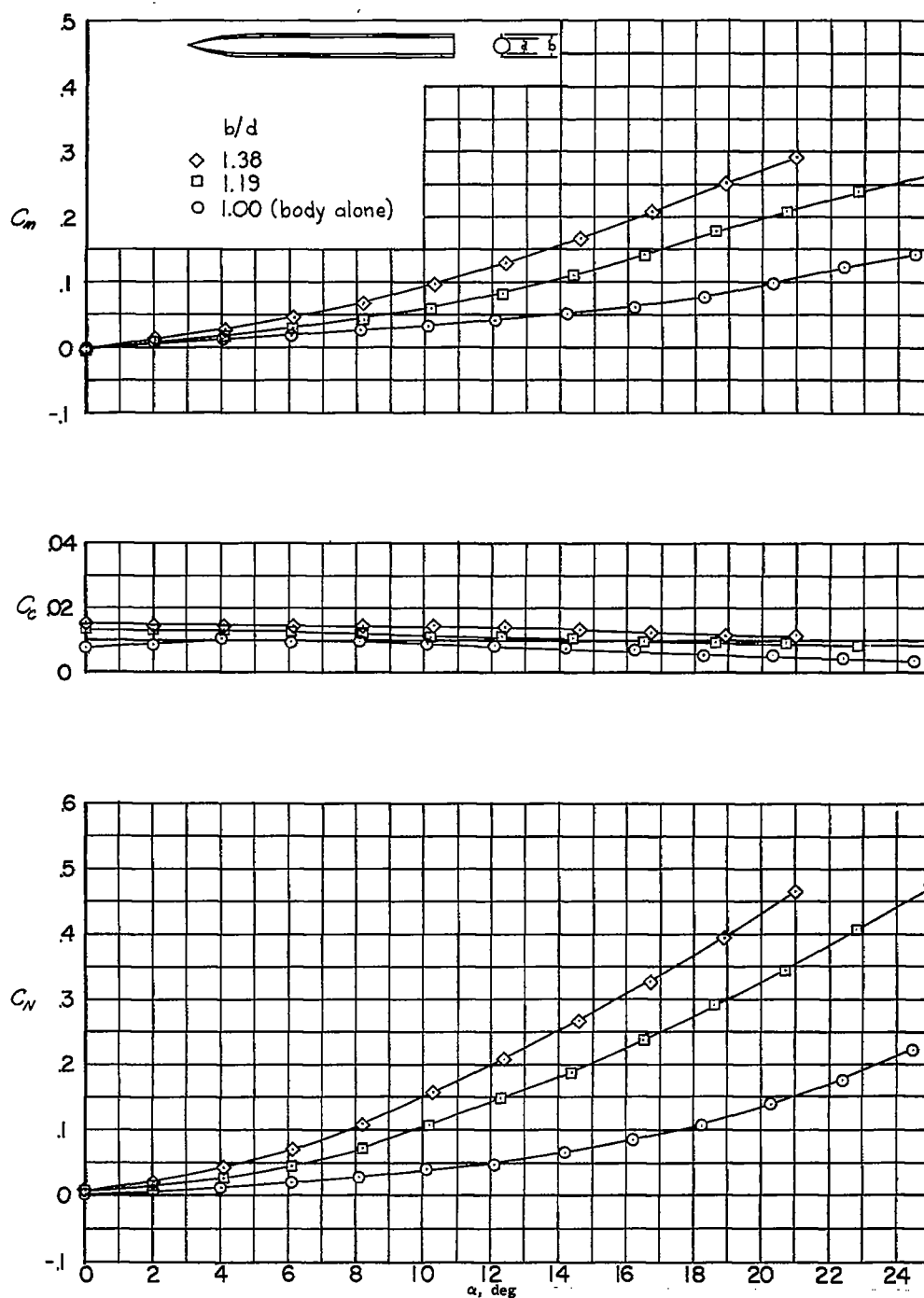
(a) $l/d = 15.7$; c.g. at $x/l = 0.60$.

Figure 9.- Effect of small span wings on the aerodynamic characteristics
in pitch of the body-alone configurations. Flagged symbols are for
$p_O = 4.0$ lb/sq in. abs; others are for $p_O = 10.7$ lb/sq in. abs.
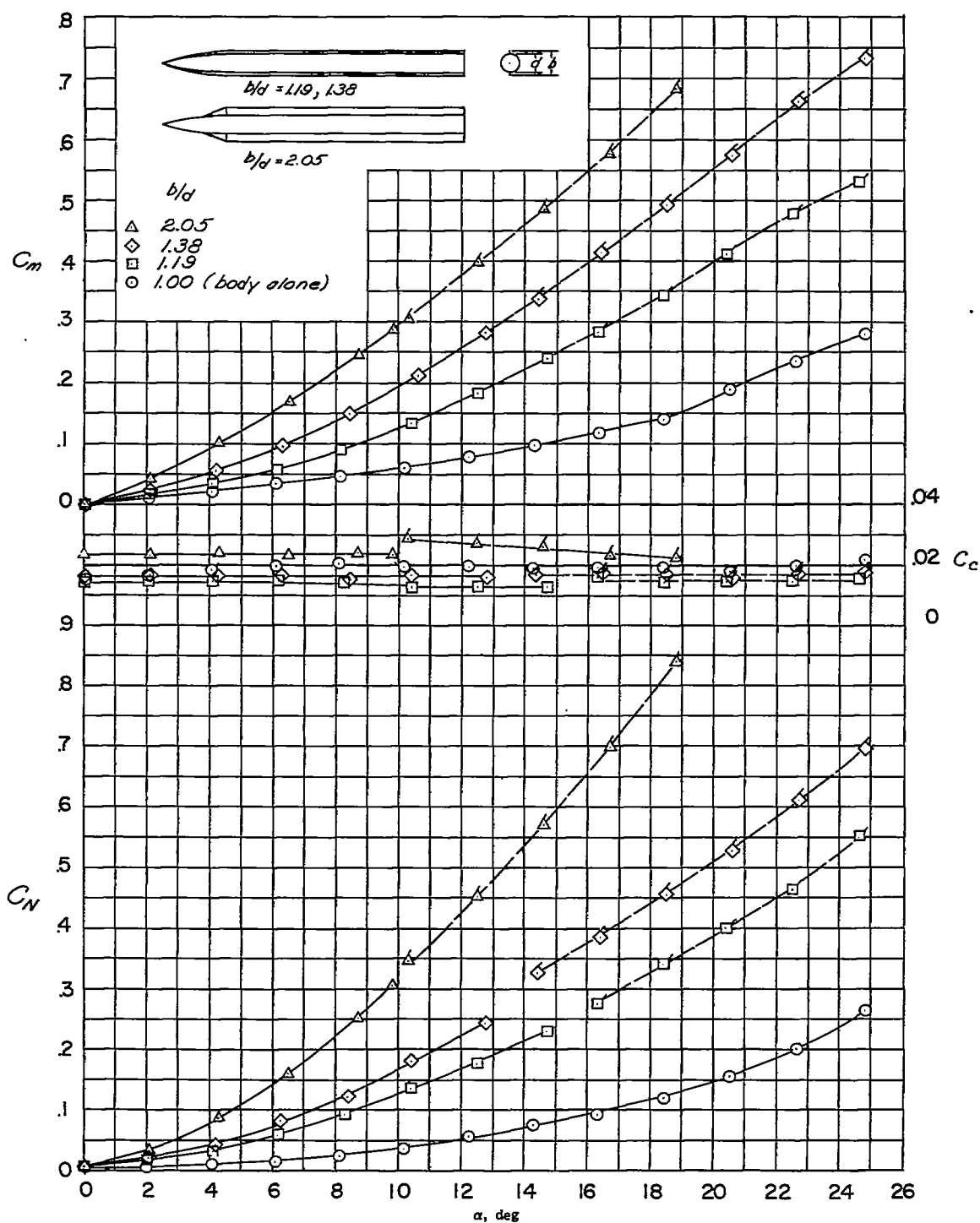
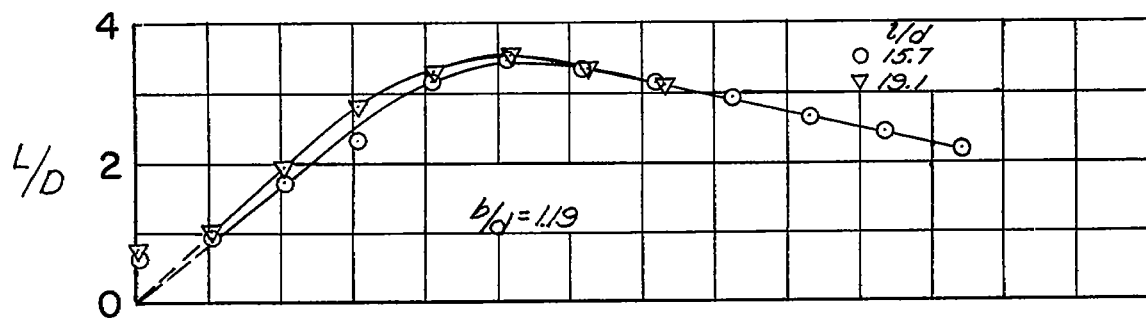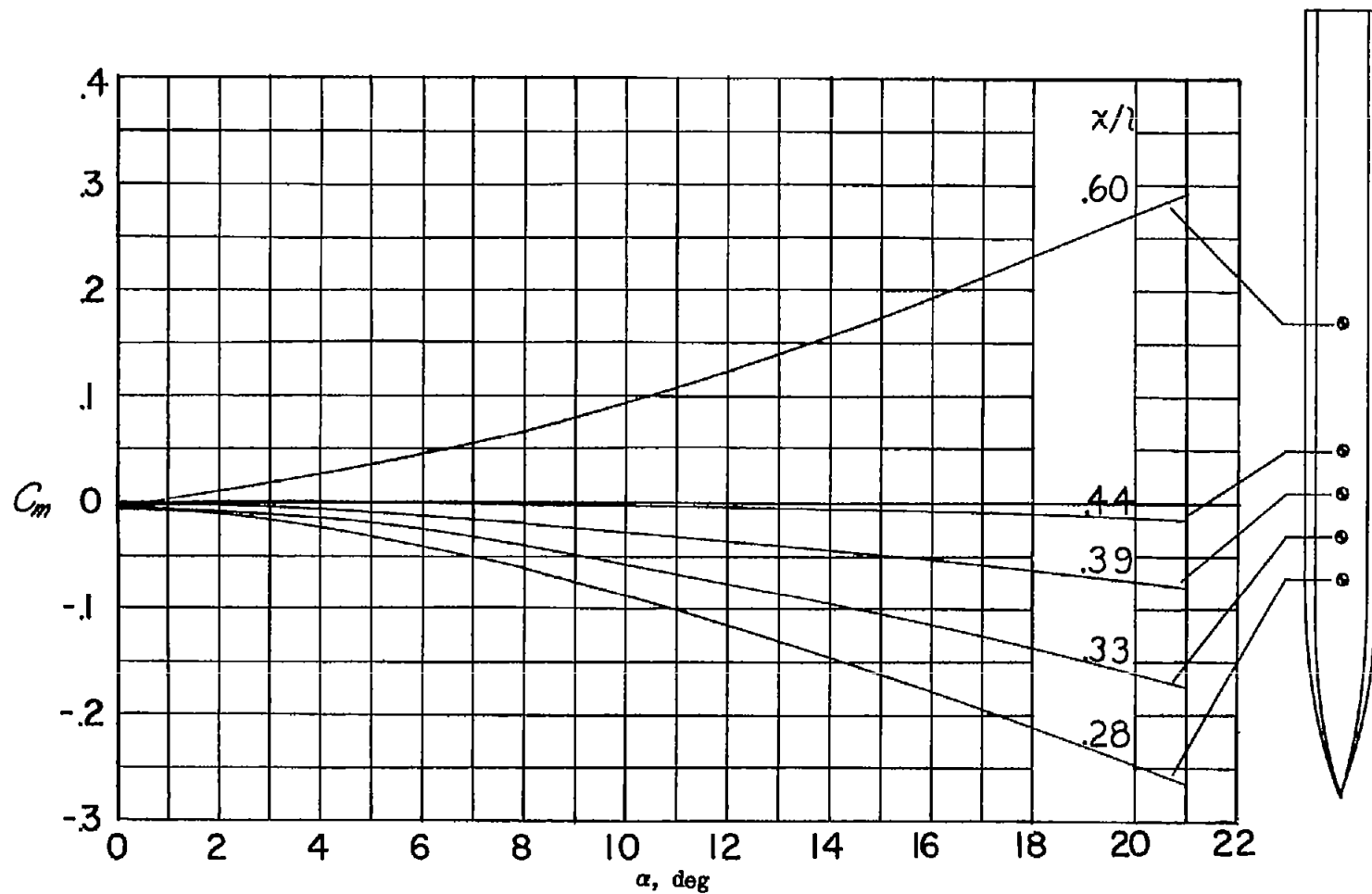(b) l/d = 19.1; c.g. at x/l = 0.67.
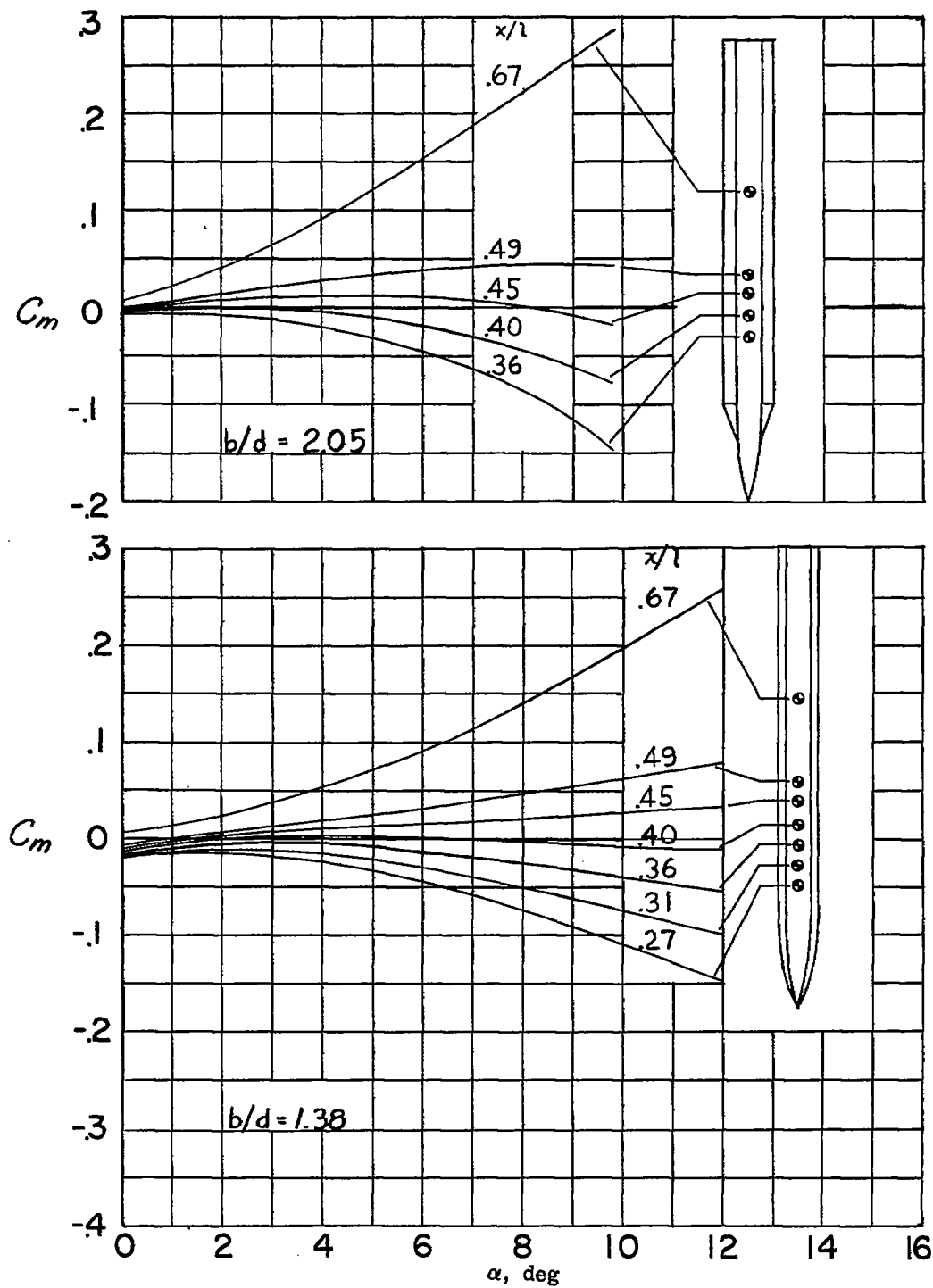
Figure 9.- Concluded.
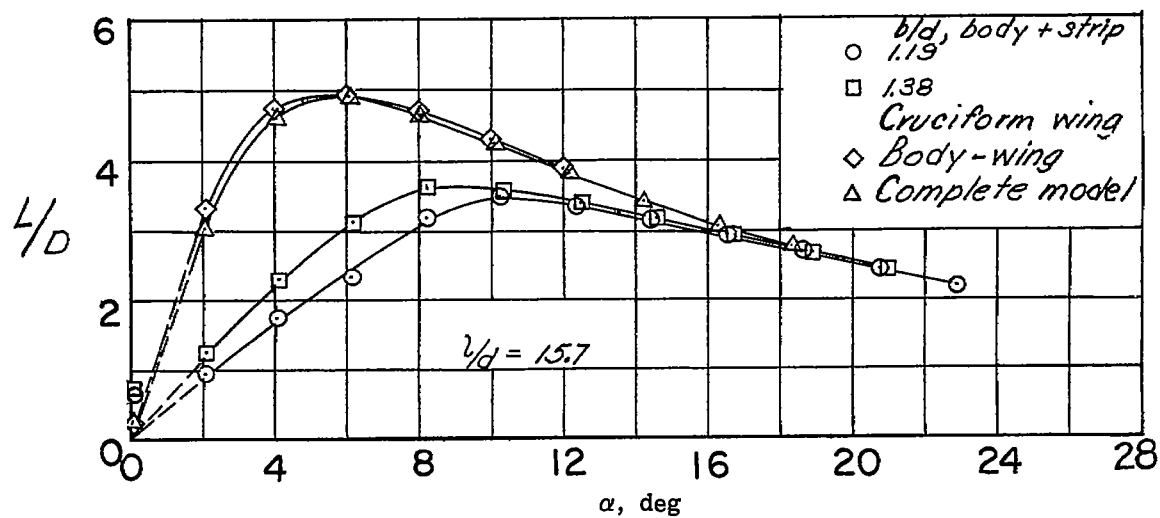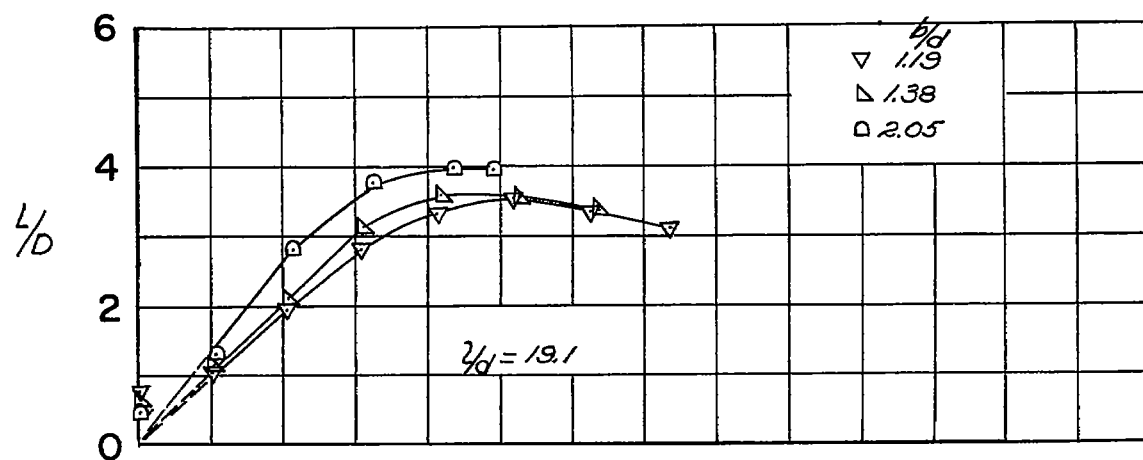
Figure 10.- Lift-drag ratios of the various configurations.

(a) $l/d = 15.7$; $b/d = 1.38$.

Figure 11.- Effect of center-of-gravity location on C_m of the body-
plus-strip configurations.

(b) $l/d = 19.1$; $b/d = 1.38$ and 2.05.
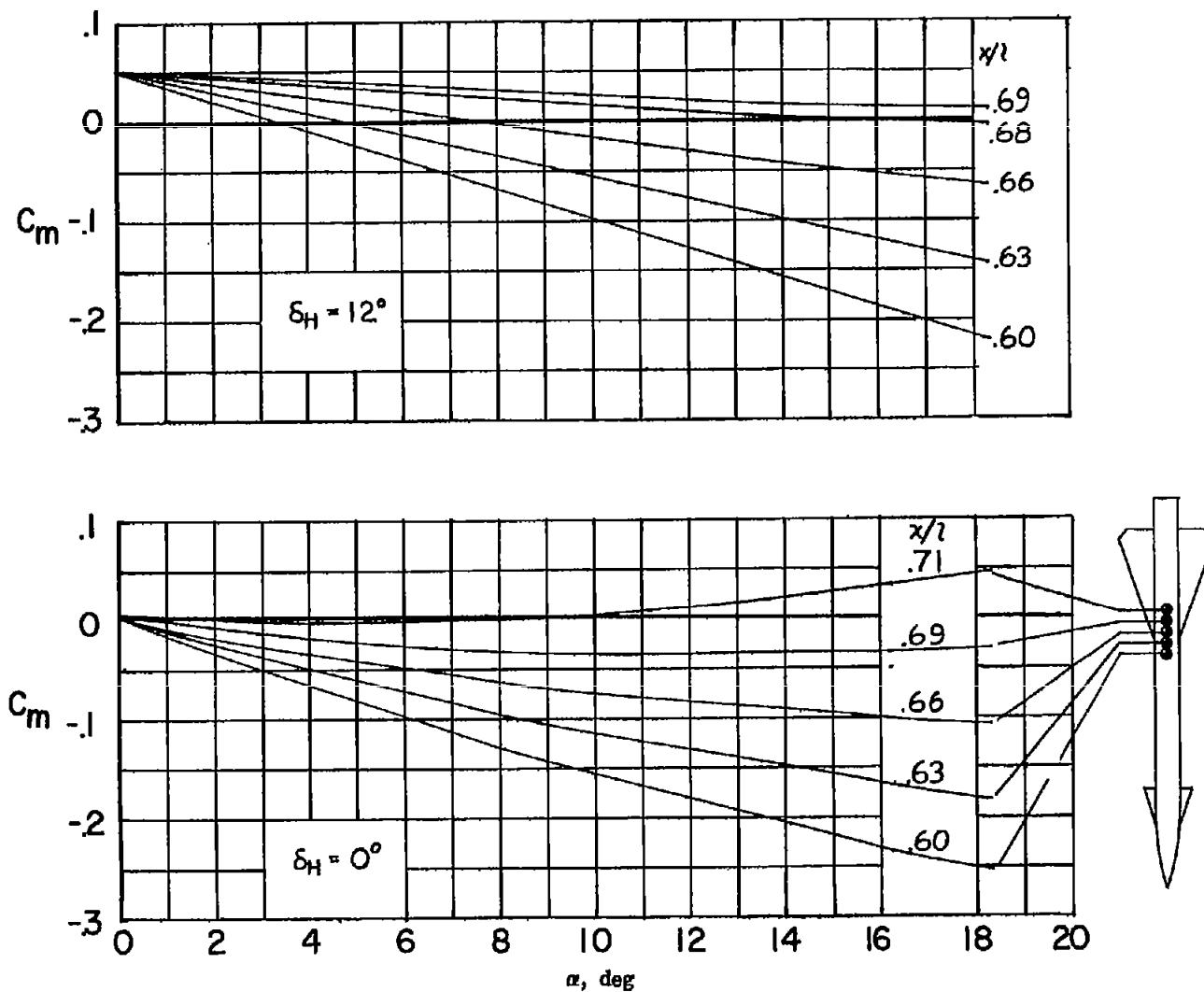
Figure 11.- Concluded.

Figure 12.- Effect of center-of-gravity location on C_m for the complete model at two horizontal-canard deflections. $l/d = 15.7$; $\phi = 0°$.